第 29 卷第 10 期 无 机 化 学 学 报 Vol.29 No.10
2013 年 10 月 CHINESE JOURNAL OF INORGANIC CHEMISTRY 2176-2182

三个基于 Cu_2X_2(X^-=Cl^-、Br^-和 I^-)结构单元双核 Cu(I)配合物的合成、晶体结构、电子吸收和发射光谱

孙晓美[1] 宁为华[1] 刘建兰*,[1] 刘少贤[1] 郭平春[1] 任小明*,[1,2]
([1]南京工业大学应用化学系,南京 210009)
([2]南京大学配位化学研究所,配位化学国家重点实验室,南京 210093)

摘要: 合成并表征了 3 个含 Cu_2X_2 结构单元的双核 Cu(I)配合物[$Cu_2(\mu$-X)$_2$(deebq)$_2$](其中 deebq=2,2′-联喹啉-4,4′-二甲酸乙酯; X=Cl (1), Br (2) or I (3))。化合物 1~3 同构,其晶体属三斜晶系,空间群为 $P\bar{1}$,具有相似的晶胞参数和晶体堆积结构。Cu_2X_2 双核单元具有反演中心对称性,每个 Cu^+与 deebq 配体中 2 个 N 原子、2 个 μ_2 桥联的卤素 X^-阴离子配位,形成扭曲的四面体配位环境。通过 deebq 配体中苯环间 $\pi\cdots\pi$ 堆积,相邻双核分子形成超分子一维链,超分子链间存在弱范德瓦尔斯引力。在二氯甲烷溶液中,3 个化合物都存在 1 个宽而不对称的电荷迁移吸收带(500~630 nm 区域),其强度和位置不受桥联 X^-配体影响。因此,电荷迁移带归属为由 Cu^+中心到 deebq 配体的电荷转移。在二氯甲烷溶液中,3 个化合物发射强荧光,发射带中心波长位于 400 nm 处,该发射带归属为 deebq 配体内的 π-π* 电子跃迁。在固体以及二氯甲烷溶液中,都没观察到从金属中心到配体的 MLCT 发射带。

关键词: 2,2′-联喹啉-4,4′-二甲酸乙酯; 双核配合物; 晶体结构; MLCT; 吸收光谱; 发射光谱
中图分类号: O614.121 **文献标识码**: A **文章编号**: 1001-4861(2013)10-2176-07
DOI:10.3969/j.issn.1001-4861.2013.00.331

Three Dinuclear Cu^+ Complexes Based on Cu_2X_2 Core (X^-=Cl^-, Br^- and I^-): Syntheses, Crystal Structures, Absorption and Emission Spectra

SUN Xiao-Mei[1] NING Wei-Hua[1] LIU Jian-Lan*,[1]
LIU Shao-Xian[1] GUO Ping-Chun[1] REN Xiao-Ming*,[1,2]
([1]*State Key Laboratory of Materials-Oriented Chemical Engineering and College of Science, Nanjing University of Technology, Nanjing* 210009, *China*)
([2]*State Key Laboratory & Coordination Chemistry Institute, School of Chemistry and Chemical Engineering, Nanjing University, Nanjing* 210093, *China*)

Abstract: Three dinuclear Cu^+ complexes [$Cu_2(\mu$-X)$_2$(deebq)$_2$] (where deebq=4,4′-diethylester-2,2′-biquinoline; X=Cl (**1**), Br (**2**) or I (**3**)), have been synthesized and characterized spectroscopically. The isostructural **1~3** crystallize in triclinic system with space group $P\bar{1}$, and show quite similar lattice parameters and packing structures. Two Cu^+ ions in a dinuclear unit are related to each other via an inversion center; each Cu^+ ion are coordinated by two N atoms form one deebq ligand and two X^- anions, which act as a μ_2-bridge mode to link two Cu^+ ions, to form a distorted tetrahedral coordination geometry. The dinuclear units are aligned into a supramolecular chain via the intermolecular $\pi\cdots\pi$ interactions between the neighboring phenyl rings in deebq ligands, and the supramolecular chains are held together through weakly intermolecular van der Waals forces.

收稿日期:2013-03-31。收修改稿日期:2013-05-07。
国家自然科学基金(No.21071080)和江苏省自然科学基金(No.BK2010551)资助项目。
*通讯联系人。E-mail:xmren@njut.edu.cn

Three complexes exhibit a broad and asymmetric absorption band in the 500~630 nm range in CH_2Cl_2, this band is almost independent on the bridged X^- ligand and not observed in the absorption spectrum of deebq in CH_2Cl_2, thus, it is assigned to MLCT from Cu^+ center to deebq ligand. Complexes **1~3** emitted intense fluorescence with the center around 400 nm, this emission band is attributed to the π-π* electronic transition of deebq ligand. No MLCT emission was observed in the CH_2Cl_2 solution and the solid state for three complexes. CCDC: 888543, **1**; 888542, **2**; 888541, **3**.

Key words: 4,4′-diethylester-2,2′-biquinoline; dinuclear complex; crystal structure; MLCT; absorption spectra; emission spectra

0 Introduction

Complexes of transition metal of low oxidation state with strong π-acceptor ligands, such as bipyridyl, phenanthroline and their derivatives, exhibit intense metal-to-ligand charge-transfer (MLCT) transitions. The MLCT state is often emissive and can be generated optically. The interest in transition metal complexes has recently intensified as a result of a wide variety of applications in solar energy conversion[1-3], chemical sensing[4-9], molecular devices[10-15] and phototherapy[16].

Monovalent Cu^+ diimine complexes have attracted increasing interest due to their various advantages, such as resource-rich, low cost and nontoxic properties, in the applications ranging from organic light emitting devices (OLEDs) to biological sensors[17] owing to their diversity structure, rich photophysical behavior and high luminescence efficiency [18]. On the other hand, the promising aspects of non-linear optical properties for quinoline derivatives were recently shown in the literatures[19], and the coordination compounds with quinoline derivative ligands may display some novel optical properties.

In this paper, we present syntheses, crystal structures and discuss absorption and emission spectra for three isostructural dinuclear Cu^+ complexes. The lowest allowed electronic transition in the absorption spectra of these complexes shows the metal-to-ligand charge transfer (MLCT) character from the d orbitals of Cu^+ to π* orbitals of the 4,4′-diethylester-2,2′-biquinoline (deebq) ligand, however, such a MLCT transition band does not appear in the emission spectra in both CH_2Cl_2 solution and solid state.

1 Experimental

1.1 Materials and methods

All chemicals were commercially available and of analytical grade, and used as received without further purification, still it must be noted that CuI was purchased from Aladdin. This ligand 4,4′-diethylester-2,2′-biquinoline (deebq) was synthesized from disodium 2,2′-biquinoline-4,4′-dicarboxylate (Na_2bqdc) following the reported process[20] and characterized by ^{1}H NMR spectrum in $CDCl_3$ with chemical shifts (δ): 9.35 (2H, s), 8.80 (2H, d), 8.35 (2H, d), 7.85 (2H, td), 7.70 (2H, td), 4.60 (4H, q, CH_2), 1.55 (6H, t, CH_3).

1.2 Physical measurements

Elemental analyses (C, H, and N) were performed with an Elementar Vario EL Ⅲ analytical instrument. Infrared (IR) spectra were recorded on a Bruker Vector 22 Fourier Transform Infrared Spectrometer (170SX) with pressed KBr pellets. ^{1}H NMR spectra were recorded on a Bruker AM-500 spectrometer at ambient temperature with chloroform-d as solvent. The UV-visible spectra were obtained from a Shimadzu UV-2450 spectrometer. Photoluminescence spectra in the dichloromethane were recorded with a Hitachi F-4600 fluorescence spectrophotometer.

1.3 Preparation of [(deebq)$_2$Cu$_2$(μ-Cl)$_2$] (1)

$CuCl_2\cdot 2H_2O$ (85 mg, 0.05 mmol) and deebq (20 mg, 0.05 mmol) together with Cu powder (2.9 mg, 0.045 mmol) were placed in a 10 cm^3 Teflon-lined digestion bomb with 2 cm^3 absolute ethyl alcohol and 5 cm^3 acetonitrile. The bomb was sealed and placed in the oven where it was heated to 100 ℃ for 48 h and then slowly cooled to ambient temperature. Deep

blue/purple single crystals were obtained by filtration in 87% yield (based on deebq). The elemental analytical calculations for $C_{48}H_{40}N_4Cl_2Cu_2O_8$(%): C, 57.71; H, 4.04; N, 5.61 and Found(%): C, 57.34; H, 4.12; N, 5.30. The main absorption bands in the infrared (IR) spectrum (KBr disk, cm^{-1}): 3 104(w) for the ν_{C-H} of the quinolyl ring; 2 977(s), 2 934(s), 2 906 (s) for the ν_{C-H} of -CH_3 and -CH_2; 1721(s) for the ν_{C-O} of the -$COOCH_2CH_3$; 1 585(m), 1 565(m), 1 509(m), 1 470 (m) for the $\nu_{C=C}$ and $\nu_{C=N}$ of the quinolyl ring; 1 264(s), 1 105(s) for the ν_{C-O-C} of the -$COOCH_2CH_3$.

1.4 Preparation of [(deebq)$_2$Cu$_2$(μ-Br)$_2$] (2)

$CuBr_2$ (12.6 mg, 0.056 mmol) and deebq (20 mg, 0.05mmol) were placed in a 10 cm^3 Teflon-lined digestion bomb with 4 cm^3 absolute ethyl alcohol and 3 cm^3 acetonitrile. The bomb was sealed and placed in the oven where it was heated to 100 ℃ for 48 h. After being slowly cooled to room temperature, black single crystals were achieved (yield 91% based on deebq). The elemental analytical calculations for $C_{48}H_{40}N_4Br_2Cu_2O_8$(%): C, 53.00; H, 3.71; N, 5.15. Found(%): C, 52.84; H, 3.83; N, 4.82. The IR spectrum (KBr disk, cm^{-1}) showed the main absorption bands: 3105 (w) for the ν_{C-H} of the quinolyl ring; 2 984(s), 2 933(s) for the ν_{C-H} of -CH_3 and -CH_2; 1721(s) for the ν_{c-o} of the -$COOCH_2CH_3$; 1 585 (m), 1 509 (m), 1 460 (m) for the $\nu_{C=C}$ and $\nu_{C=N}$ of the quinolyl ring; 1 265(s), 1 109(s) for the ν_{C-O-C} of the -$COOCH_2CH_3$.

1.5 Preparation of [(deebq)$_2$Cu$_2$(μ-I)$_2$] (3)

A mixture of CuI (9.5 mg, 0.05 mmol), KI (48.6 mg, 0.05 mmol) and deebq (20 mg, 0.05 mmol) together with absolute ethyl alcohol (7 cm^3) were sealed in a 10 cm^3 Teflon lined reactor and heated at 100 ℃ for 48 h, and then cooled slowly to room temperature. Black single crystals were obtained directly in 92% yield. The elemental analytical calculations for $C_{48}H_{40}N_4I_2Cu_2O_8$ (%): C, 48.78; H, 3.41; N, 4.76. The experimental values included the following (%): C, 49.00; H, 3.46; N, 4.68. The IR spectrum (KBr disk, cm^{-1}) showed the main absorption bands: 3 099 (w) for the ν_{C-H} of the quinolyl ring; 2 982(s), 2 932(s) for the ν_{C-H} of -CH_3 and -CH_2; 1 721(s) for the ν_{c-o} of the -$COOCH_2CH_3$; 1 586 (m), 1 508 (m), 1 460 (m) for the $\nu_{C=C}$ and $\nu_{C=N}$ of the quinolyl ring; 1 264(s), 1 105(s) for the ν_{C-O-C} of the -$COOCH_2CH_3$.

1.6 X-ray single crystallography

The single crystal X-ray diffraction data were collected for **1**~**3** at 296 K with graphite monochromated Mo $K\alpha$ (λ=0.071 073 nm) on a CCD area detector (Bruker-SMART). Data reductions and absorption corrections were performed with the SAINT and SADABS software packages, respectively[21]. Structures were solved by a direct method using the SHELXL-97 software package[22]. The non-hydrogen atoms were anisotropically refined using the full-matrix least-squares method on F^2. All hydrogen atoms were placed at the calculated positions and refined riding on the parent atoms. The details about data collection, structure refinement and crystallography are summarized in Table 1.

CCDC: 888543, **1**; 888542, **2**; 888541, **3**.

Table 1 Crystal and structural refinement data for 1~3

Compound	**1**	**2**	**3**
Chemical formula	$C_{48}H_{40}N_4Cl_2Cu_2O_8$	$C_{48}H_{40}N_4Br_2Cu_2O_8$	$C_{48}H_{40}N_4I_2Cu_2O_8$
Formula weight	998.84	1 087.74	1 181.74
T / K	296(2)	296(2)	296(2)
Wavelength / nm	0.071 073	0.071 073	0.071 073
Space group	$P\bar{1}$	$P\bar{1}$	$P\bar{1}$
a / nm	0.860 88(16)	0.860 90(12)	0.867 08(14)
b / nm	1.126 4(2)	1.128 99(15)	1.135 97(18)
c / nm	1.278 4(2)	1.290 48(18)	1.312 7(2)
α / (°)	105.238(2)	104.403(2)	103.404(2)
β / (°)	107.124(2)	108.025(2)	108.587(2)

Continued Table 1

γ / (°)	102.076(2)	101.690(2)	101.570(2)
V / nm^3	1.086 4	1.100 7	1.138 1
Z	3	3	3
D_c / (g·cm^{-3})	1.527	1.641	1.724
F(000)	512	548	584
Abs. coeff. / mm^{-1}	1.163	2.841	2.349
θ ranges of data collection / (°)	1.78~27.54	1.76~27.40	1.73~27.49
Index ranges	$-10 \leqslant h \leqslant 11$, $-14 \leqslant k \leqslant 14$, $-16 \leqslant l \leqslant 15$	$-10 \leqslant h \leqslant 11$, $-14 \leqslant k \leqslant 12$, $-16 \leqslant l \leqslant 16$	$-11 \leqslant h \leqslant 11$, $-14 \leqslant k \leqslant 14$, $-16 \leqslant l \leqslant 17$
Reflections collected	9 625	9 612	9 491
R_{int}	0.031 6	0.023 4	0.036 1
Independent reflections	5 015	5 001	5 225
Refinement method on F^2	Full-matrix least-squares		
Goodness of fit on F^2	1.027	1.031	1.051
Final R indices ($I>2\sigma(I)$)	R_1=0.042 3, wR_2=0.105 5	R_1=0.034 3, wR_2=0.069 6	R_1=0.041 1, wR_2=0.104 4
R indices (all data)	R_1=0.073 4, wR_2=0.123 9	R_1=0.058 0, wR_2=0.085 2	R_1=0.055 3, wR_2=0.118 5
Residual / (e·nm^{-3})	339 / −422	332 / −410	589 / −822

$R_1=\sum||F_o|-|F_c||/|F_o|$, $wR_2=[\sum w(F_o^2-F_c^2)^2/\sum w(F_o^2)^2]^{1/2}$.

2 Results and discussion

2.1 Descriptions of crystal structures

Complexes **1**~**3** are isostructural to each other and their crystals belong to triclinic space group $P\bar{1}$. Three complexes show quite similar lattice parameters (Table 1) and analogous molecular packing structure, however, their bond lengths and angles are different, typical bond lengths and bond angles are summarized in Table 2.

As shown in Fig.1, an asymmetric unit of **1** consists of one Cu^+ ion, one Cl^- anion together with one deebq ligand. Two equivalent Cu(deebq) units are connected by two Cl^- anions in μ_2-bridged mode to form a dimer, with ∠Cu-Cl-Cu=77.79 (3)°and $d_{Cu\cdots Cu}$= 0.296 0 nm. The dimer possesses an inversion center, which coincides with the midpoint of the Cu ⋯ Cu vector. Two Cu-N bond lengths, 0.206 7(2) and 0.208 1(2) nm, are close to each other and fall within the expected range, while two Cu-Cl lengths, 0.226 00(8) and 0.244 84(9) nm, show significant difference; the ∠Cl-Cu-Cl=102.21(3)°, whereas the ∠N-Cu-N bite angle is 79.74(8)°, which is much deviate from the ideal

Table 2 Typical bond lengths (nm) and angles (°) in the Cu_2X_2 core of 1~3

	1	2	3
N1-Cu1	0.206 7(2)	0.208 1(2)	0.208 7(3)
N2-Cu1	0.208 1(2)	0.208 5(2)	0.210 6(3)
Cu1-X1	0.226 00(8)	0.239 53(6)	0.256 80(7)
Cu1-X1#1	0.244 84(9)	0.253 46(6)	0.266 10(7)
N1-Cu1-N2	79.74(8)	79.51(9)	79.45(13)
N2-Cu1-X1	126.71(6)	125.40(7)	123.69(10)
X1-Cu1-X1#1	102.21(3)	105.61(2)	108.28(2)
N1-Cu1-X1#1	109.69(7)	109.31(7)	108.89(9)
Cu1-X1-Cu1#1	77.79(3)	74.39(2)	71.72(2)

Symmetry codes: #1: −*x*+1, −*y*+2, −*z*+2 (**1**); #1: −*x*+1, −*y*+2, −*z*+2 (**2**); #1: −*x*+1, −*y*+2, −*z*+2 (**3**).

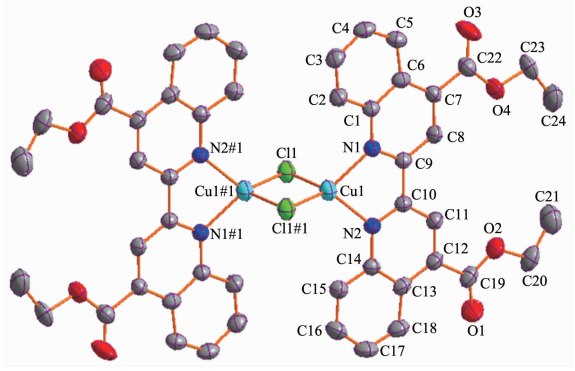

Symmetry codes: #1: −*x*+1, −*y*+2, −*z*+2

Fig.1 ORTEP view of **1** with non-hydrogen atom labeling and thermal ellipsoids at 50% probability level

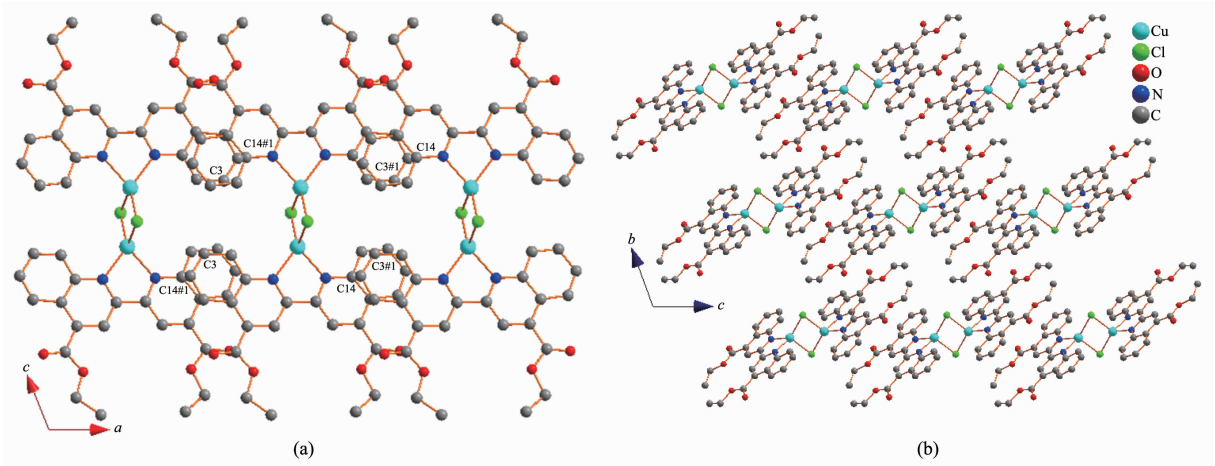

Hydrogen atoms removed for clarity

Fig.2 (a) A supramolecular chain via intermolecular $\pi\cdots\pi$ interactions (b) the view of the packing of **1** along the *a*-axis direction

tetrahedral angle (109.27°), in the distorted tetrahedral CuN_2Cl_2 coordination sphere. In addition, the five-membered chelate ring adopts an envelope conformation with the Cu^+ deviating from the mean molecule plane N(1)C(9)C(10)N(2) by 0.030 9 nm. The molecule planes of two biquinoline ligands are parallel but are shifted with respect to each other in such a way that they form a stair motif with the interplane distance of 0.222 8 nm. This shift is apparently associated with the tendency to reduce the steric repulsion between the hydrogen atoms of adjacent ligands[23-25].

The $Cu_2(deebq)_2Cl_2$ dimers are aligned into a supramolecular chain along the *a*-axis direction via the intermolecular $\pi\cdots\pi$ interactions between the neighboring phenyl rings of biquinolines, with the shortest C···C contact 0.336 8 nm between C3 and C14#1 (the hash-marked atom is symmetrically generated with the symmetric code #1 $-x+1$, $-y+2$, $-z+2$), the distance 0.323 0 nm between the mean-molecule planes of overlapped phenyl rings and the centroid-to-centroid distance 0.370 6 nm (ref. Fig.2a). The supramolecular chains are held together through weakly intermolecular van der Waals forces (ref. Fig. 2b).

2.2 UV-visible absorption and photoluminescence spectra

The UV-Vis absorption spectra of **1**~**3** in CH_2Cl_2 (with concentration $c=2.5\times10^{-5}$ mol·L^{-1}), which are quite similar to each other, are displayed in Fig.3 together with the UV-Vis absorption of the deebq ligand; the wavelength λ_{max} and the corresponding ε values of the absorption bands are summarized in Table 3. Three intense absorption bands in the

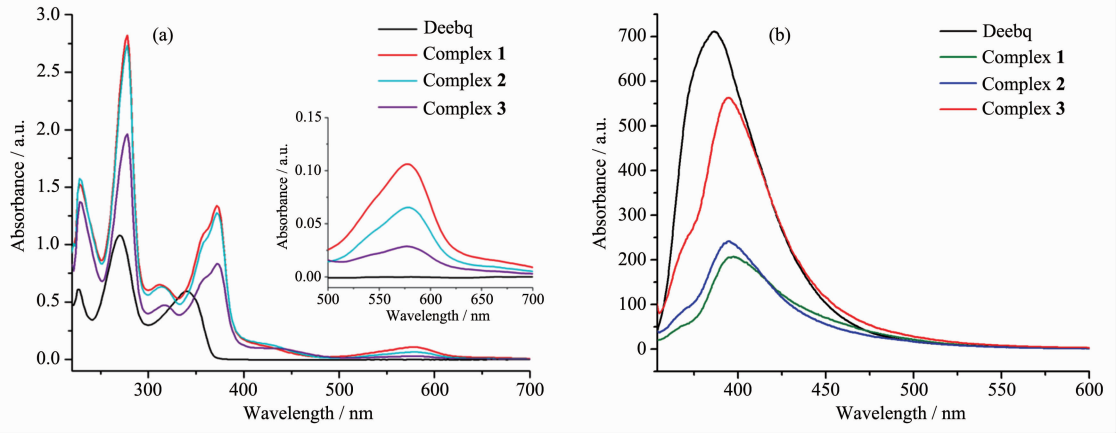

Fig.3 (a) Absorption and (b) emission spectra of **1**~**3** with deebq in CH_2Cl_2 at ambient temperature

Table 3 Wavelength λ_{max} (nm) and the corresponding ε ($L\cdot mol^{-1}\cdot cm^{-1}$) value for the absorption bands in the spectra of 1~3 and the deebq ligand

	λ_{max}, ε				
	Band Ⅰ	Band Ⅱ	Band Ⅲ	Band ⅠⅣ	Band Ⅴ
1	228, 60 960	278, 112 840	312, 26 000	372, 53 640	578, 4 320
2	228, 63 040	278, 109 440	314, 25 320	372, 51 120	578, 2 640
3	228, 54 840	278, 78 520	318, 18 920	372, 33 320	578, 1 160
deebq	226, 24 400	270, 43 280	340, 23 720		

spectrum of the deebq ligand and four intense absorption bands with two shoulders in the spectra of **1**~**3** are observed in 200~400 nm region, these absorption bands could be assigned to π-π* electronic transitions within the deebq ligand[26]. It is notable that **1**~**3** exhibit a broad and asymmetric absorption band in the 500~630 nm range, and this band results in the deep purple color of three compounds. Moreover, the maximum of the of the asymmetric absorption bands are independent on the halogen anion in **1**~**3**, as a result, such a band can be attribute to MLCT transition from Cu^+ center to deebq ligand[25,27-28].

It is well known that the metal-organic polymeric complexes with d^{10} closed-shell electronic configuration exhibit generally the intense emission fluorescence that arises from the intra-ligand π-π* or MLCT/LMCT charge transfer transition[29-31]. The emission spectra of **1**, **2** and **3** (with $c=10^{-4}$ mol·L^{-1}) at room temperature are measured and shown in Fig.3b together with the deebq for comparison. Complexes **1**~**3** display an emission band, which maximum locates at 398, 395 and 395 nm, respectively. The deebq gives its emission band with the maximum of peak at 387 nm, upon excitation at 294 nm. However, the 2,2′-biquinoline-4,4′-dicarboxylic acid (H_2bqdc) exhibits a strong and broad emission at 430 nm upon excitation at 260 nm in solid state [24]. In addition, the salt K_2bqdc shows one weak emission band at 402 nm upon excitation at 260 nm[32]. Thus, it is suggested that the emission band centered on ~400 nm in the fluorescence spectra of **1**, **2** and **3** originates from the π-π* electronic transition of deebq ligand, and the emission originated from MLCT transition was not observed in the CH_2Cl_2 solution and the solid state for three dinuclear complexes.

3 Conclusions

In summary, three new dinuclear coordination compounds based on deebq were successfully synthesized under different hydrothermal conditions. The crystals of **1**, **2** and **3** are isostructural with very similar lattice parameters and packing structures. The dinuclear units are aligned into a supramolecular chain via the intermolecular $\pi\cdots\pi$ interactions between the neighboring phenyl rings of biquinolines in the crystal. The supramolecular chains are held together through weakly intermolecular van der Waals forces. The lowest allowed electronic transition in the absorption spectra of three compounds shows $Cu^+\longrightarrow$ deebq MLCT character. Three dinuclear compounds show intense emission with the maximum of the emission band at ~400 nm in CH_2Cl_2 solution due to the intraligand π-π* transition, however, the emission originated from MLCT is not observed in both the solution and solid state for three dinuclear compounds. In addition, the intense emission near the 400 nm suggests these compounds have a potential application in fluorescence materials.

Acknowledgements: Authors thank the Science and Technology Department of Jiangsu Province and National Natural Science Foundation of China for financial support (grant nos. BK2010551 and 21071080).

References:

[1] Ruthkosky M, Kelly C A, Zaros M C, et al. *J. Am. Chem. Soc.*, **1997**,**119**:12004-12005

[2] Bignozzi C A, Argazzi R, Kleverlaan C, et al. *J. Chem. Soc. Chem. Rev.*, **2000**,**29**:87-96

[3] George B S, Christian D G, Hideaki S, et al. *J. Am. Chem. Soc.*, **2007**,**129**:2147-2160

[4] Thanasekaran P, Liao R T, Liu Y H, et al. *Coord. Chem. Rev.*, **2005**,**249**:1085-1110

[5] Vannelli T A, Karpishin T B. *Inorg. Chem.*, **2000**,**39**:1336-1336

[6] Melinda H K, Kurt D B, Joseph T H, et al. *Coord. Chem. Rev.*, **2000**,**205**:201-228

[7] De S A P, Fox D B, Moody T S, et al. *Pure Appl. Chem.*, **2001**,**73**:503-511

[8] Rudzinski C M, Nocera D G. *Mol. Supramol. Photochem.*, **2001**,**7**:1-3

[9] Kapturkiewicz A. *Electrochemistry of Functional Supramolecular Systems*. Hoboken NJ: John Wiley & Sons, **2010**:477

[10]Armaroli N, Balzani V, Barigelletti F, et al. *J. Am. Chem. Soc.*, **1994**,**116**:5211-5217

[11]Baldo M A, O′Brien D F, You Y, et al. *Nature*, **1998**,**395**:151-154

[12]Baldo M A, Thompson M E, Forrest S R, et al. *Nature*, **2000**,**403**:750-753

[13]Collin J P, Dietrich-Buchecker C, Gavina P, et al. *Acc. Chem. Res.*, **2001**,**34**:477-487

[14]Sauvage J P. *Science*, **2001**,**291**:2105-2106

[15]Li M Z, Bin L, Zhong M S, et al. *J. Phys. Chem. C*, **2009**, **113**:13968-13973

[16]Ali H, Van Lier J E. *Chem. Rev.*, **1999**,**99**:2379-2450

[17](a)Zhang Q S, Ding J Q, Cheng Y X, et al. *Adv. Funct. Mater.*, **2007**,**17**:2983-2990

(b)Moudam O, Kaeser A, Delavaux-Nicot B, et al. *Chem. Commun.*, **2007**,**1**:3077-3079

(c)Zhang Q S, Zhou Q G, Cheng Y X, et al. *Adv. Funct. Mater.*, **2006**,**16**:1203-1208

(d)Armaroli N, Accorsi G, Holler M, et al. *Adv. Mater.*, **2006**,**18**:1313-1316

(e)Zhang Q S, Zhou Q G, Cheng Y X, et al. *Adv. Mater.*, **2004**,**16**:432-436

[18](a)Kyle K R, Ryu C K, Dibenedetto J A, et al. *J. Am. Chem. Soc.*, **1991**,**113**:2954-2965

(b)Kim T H, Shin Y W, Jung J H, et al. *Angew. Chem. Int. Ed.*, **2008**,**47**:685-688

(c)Tran D, Bourassa J L, Ford P C, et al. *Inorg. Chem.*, **1997**,**36**:439-442

(d)Vitale, M, Ford P C. *Coord. Chem. Rev*., **2001**,**219**:3-16

(e)De Angelis F, Fantacci S, Sgamellotti A, et al. *Inorg. Chem.*, **2006**,**45**:10576-10584

[19]Makowska-Janusik M, Gondek E, Kityk I V, et al. *Chem. Phys.*, **2004**,**306**:265-271

[20]Hoertz P G, Staniszewski A, Marton A, et al. *J. Am. Chem. Soc.*, **2006**,**128**:8234-8245

[21]*Bruker, SAINT* (*Version* 6.22) *and SMART* (*Version* 5.625), Bruker AXS Inc., Madison, WI, USA, **2001**.

[22]Sheldrick G M. *SHELXL*-97, *Program for the Refinement of Crystal Structure*; University of Göttingen, Göttingen, Germany, **1997**.

[23]Butcher R J, Sinn E. *Inorg. Chem.*, **1977**,**16**:2334-2343

[24]Sinn E. *J. Chem. Soc. Dalton Trans.*, **1976**,**7**:162-165

[25]Vatsadze S Z, Dolganov A V, Yakimanskii A V, et al. *Russ. Chem. Bull. Int. Ed.*, **2010**,**4**:710-718

[26]Ye J W, Zhang P, Ye K Q, et al. *J. Solid State Chem.*, **2006**,**179**:438-449

[27]Jahng Y, Hazelrigg J, Kimball D, et al. *Inorg. Chem.*, **1997**, **36**:5390-5395

[28]Ali B F, Al-Sou′od K, Al-Ja′ar N, et al. *J. Coord. Chem.*, **2006**,**59**:229-241

[29]Shi X, Zhu G, Wang X, et al. *Cryst. Growth Des.*, **2005**,**5**:341-346

[30]Wang X L, Qin C, Wang E, et al. *Inorg. Chem.*, **2004**,**43**:1850-1856

[31]Shan X C, Jiang F L, Yuan D Q, et al. *Dalton Trans.*, **2012**, **41**:411-416

[32]Chen X L, Wang J J, Hu H M, et al. *Z. Anorg. Allg. Chem.*, **2007**,**633**:2053-2058